

RESEARCH ARTICLE

# Novel synthetic LPDs consisting of different cholesterol derivatives for gene transfer into hepatocytes

Jiao Lu\*, Di Zhu\*, Zhi-Rong Zhang, Li Hai, Yong Wu, and Xun Sun

Key Laboratory of Drug Targeting and Drug Delivery Systems, Ministry of Education, West China School of Pharmacy, Sichuan University, Chengdu, Sichuan, P.R. China

## Abstract

In the present study, LPDs composing of a series of novel synthetic cholesterylated derivatives bearing a cluster of galactose residues and different spacer lengths were prepared for performing target gene delivery to hepatocytes and their physiochemical properties as well as gene transfer efficiency were investigated. In agreement with the “clustering effect” known to occur with more complex oligomeric structures, the addition of galactose residues under optimized spatial arrangement condition invariably increased the transfect efficiency into hepatoma cells, which can be owed to the sufficient binding of galactose ligands to the ASGPR on hepatocytes. However, the gene transfer ability to hepatocytes was not always improved with extended spacer arms, suggesting a spatial binding sites arrangement of the receptor. Moreover, our research has established galactosylated LPDs, specifically, LPDIIb, LPDIIIc, and LPDIVe as potential vectors to deliver special genes into hepatocytes with low toxicity, combining the condensing effect of protamine and the targeting capability of cholesterylated thiogalactosides.

**Keywords:** ASGPR; galactosylated LPD; cholesterylated thiogalactosides; hepatotrophic gene targeting

## Introduction

One of the most successful cationic lipids based gene delivery system reported to date is liposomes/protamine/DNA (LPD), known for their superior gene transfer ability over conventional liposomes (Li et al., 1998; Sorgi, Bhattacharya, & Huang, 1997; Li & Huang, 1997; Gao & Huang, 1996). For targeting purposes, LPD was incorporated with cell- or tissue-specific ligands as an effective approach to improve gene transfer efficiency in target tissue or cells. Among those ligands, galactose is the most extensively studied to target genes to liver parenchymal cells since galactose moiety can be specifically recognized by asialoglycoprotein receptors (ASGPR) on hepatocytes (Schwartz et al., 1981).

The affinity and specificity of the ASGPR is a consequence of oligovalent interactions with its physiological ligands, a process termed “cluster glycoside effect” by Lee et al. (1983). The receptor consists of two homologous

subunits, designated H1 and H2 in the human system, which form a noncovalent heterooligomeric complex with an estimated ratio of 2-5:1, respectively. Both subunits are single-spanning membrane proteins with a calcium-dependent galactose/*N*-acetyl-gal-actosamine recognition domain (Bider et al., 1996). Recently, the X-ray crystal structure of the carbohydrate recognition domain (CRD) of the major subunit H1 was elucidated (Meier et al., 2000).

Many studies have been performed with both natural and synthetic carbohydrates to establish the structure-affinity relationship for the ASGPR. Baenziger et al. (Baenziger & Fiete, 1980; Baenziger & Maynard, 1980) have shown that the human receptor exhibits specificity for terminal Gal and GalNAc (with an approximately 50-fold higher affinity for the latter) on desialylated glycoproteins. Triantennary ligands displayed a higher affinity than their mono- and diantennary counterparts. Furthermore, the studies led to the conclusion that only

\*These authors contributed equally to this work.

Address for Correspondence: Xun Sun, Key Laboratory of Drug Targeting and Drug Delivery Systems, Ministry of Education, West China School of Pharmacy, Sichuan University, Chengdu, Sichuan, P.R. China; E-mail: xunsun22@gmail.com

(Received 09 October 2009; revised 26 November 2009; accepted 01 December 2009)

the terminal residues are necessary for specific recognition, and that the binding process proceeds through a simultaneous interaction of 2–3 sugar residues with 2–3 binding sites of the heterooligomeric receptor (Khorev et al., 2008). Studies on rabbit hepatocytes by Lee et al. (Lee et al., 1983; Conolly et al., 1982) using synthetic oligosaccharides, further reinforced the binding hierarchy of polyvalent ligands: tetraantennary > triantennary >> diantennary >> monoantennary (Khorev et al., 2008). The optimal distance of the Gal moieties in these oligosaccharides was determined by binding assays with synthetic carbohydrates representing partial structures of N-linked glycans (Khorev et al., 2008) high-resolution NMR, and molecular modeling studies (Bock, Arnarp, & Lönngrén 1982). Based on these results, Lee et al. (Lee et al., 1983; Khorev et al., 2008) presented a model for the optimal spatial arrangement of the terminal sugar residues (Khorev et al., 2008).

Despite attempts made to elucidate the correlation between the structural differences of the ligands and their binding affinity to the receptor; the frequently used methods to construct multivalent structures include conjugation of carbohydrate ligands with proteins (i.e., neoglycoproteins) or other polymers (Stowell & Lee, 1980; Pazur, 1981), polymerization of glycosylated monomers (i.e., glycopolymers) (Horejsí, Smolek, & Kocourek, 1978; Roy, Tropper, & Romanowska, 1992) and formation of liposomes using glycolipids or neoglycolipids. As for liposomes, how the variability in ligands' structures on its surface influences its specific gene transfer ability when conjugated with gene delivery vectors has been rarely discussed. Besides, although these approaches have been successful, the products are ambiguous in composition and structure (Eggen et al., 1989; Stoll et al., 1988); the basic knowledge of the structure-activity relationship is still unsatisfactory and the optimization of these systems remains largely a result of trial and error (Masotti et al., 2009).

Therefore, it is in our study that the galactosylated cholesterol bearing a cluster of galactose residues and different spacer lengths were synthesized and the possible relation between the structural diversity of LPD and its gene transfer ability was investigated for the first time.

In our previous study, cholesterylated thiogalactosides bearing different spacer lengths were synthesized to formulate LPD complexes and the lipid-protamine-DNA complex containing cholesterylated thiogalactoside 1c (Sun et al., 2005) was established as the most promising vector for hepatocyte-specific gene delivery *in vitro* among LPDs, combining the condensing effect of protamine and the targeting capability of cholesterylated thiogalactosides. However, several questions remain unclear concerning other structural factors especially the amount of galactosidase moieties that might attribute to the affinity between ASGPR and its ligands on LPDs,

which result in the variability in their gene transfer efficiency. To further clarify the unaddressed problems, we prepared a series of Gal-LPDs composing cholesterylated thiogalactosides possessing different galactose densities and spacer lengths and studies on those Gal-LPDs were investigated such as characterization, *in vitro* gene transfer study and cell viability, etc., which might prove valuable in optimizing the strategy for hepatotrophic gene targeting.

## Materials and methods

### Materials

The plasmid pORF lacZ (3.54kb) was purchased from Invitrogen (USA). Protamine sulfate (derived from salmon), dimethyldioctadecyl ammonium bromide (DDAB) and dioleoylphosphatidylethanol-amine (DOPE) were purchased from Sigma. Qiagen Giga Endo-free plasmid purification kit was purchased from Qiagen (CA, USA). Cell culture medium RPMI-1640 was obtained from Gibco Co. (USA). Lipofectamine™ 2000 Transfection Reagent and  $\beta$ -gal assay kit were from Invitrogen (USA). Mouse fibroblasts L929, Hepatoma cells HepG2 and A549 were obtained from Shanghai Cell Institute, China Academy of Sciences. All the other chemicals and reagents used were of the analytical grade obtained commercially.

### Synthesis of galactosylated cholesterols

#### Synthesis of target compound IIa–f (Figure 1, Scheme 1C)

Cholesterol was methylsulfonylated, followed by coupling with the corresponding oligo-polyethylene glycol, yielding the intermediate 3a. According to previous methods (Loiseau, Hii, & Hill, 2004; Burns et al., 1999), using 2,3-dihydro-2H-pyran to protect one hydroxyl functionality, the other hydroxyl group of triethylene glycol was sulfonylated with methylsulfonyl chloride, leading to the mono-mesylate-ester 6, which was subsequently coupled with the intermediate 3a, affording the compound 7a. After deprotection of 7a, the target compound 3d (Scheme 1B) bearing the prolonged oligo-diethylene glycol chain was achieved. To prepare the potential scaffold 9a, 3a was sulfonylated with methylsulfonyl chloride, resulting in the compound 8a, which can convert into iodide 9a via substitution of the mesyl group by NaI in refluxing butanone. By conjugation of 9a with the known 2,3,4,6-tetra-*O*-acetyl-1-thio- $\beta$ -D-galacto-pyranose, using diisopropylethylamine (DIPEA) as catalyst, the monosaccharide derivative 11a was achieved. After deacetylation under mild condition, the desired product IIa was yielded. Compound IIa (C<sub>37</sub>H<sub>64</sub>O<sub>7</sub>S): <sup>1</sup>HNMR ( $\delta$  ppm, 400 MHz, CD<sub>3</sub>OD): 5.36 (m,

1H, chol H-6), 4.35–3.43 (13H, gal. protons and  $4 \times \text{CH}_2\text{O}$ ), 3.19 (m, 1H, chol H-3), 2.94 (m, 1H, SCH-a), 2.81 (m, 1H, SCH-b), 2.39–0.71 (remaining chol protons) with 1.01 (s, 3H,  $\text{CH}_3$ -19), 0.93 (d, 3H,  $\text{CH}_3$ -21,  $J_{20,21} = 6.4$  Hz), 0.87 (d, 6H,  $\text{CH}_3$ -26 and  $\text{CH}_3$ -27,  $J_{25,26} = J_{25,27} = 6.8$  Hz), 0.71 (s, 3H,  $\text{CH}_3$ -18). MS ( $m/z$ ): ( $\text{M} + \text{Na}$ )<sup>+</sup> 675.

The synthetic route of compound IIb-f is similar to that of compound IIa. Compound IIb ( $\text{C}_{39}\text{H}_{68}\text{O}_8\text{S}$ ): <sup>1</sup>HNMR ( $\delta$  ppm, 400 MHz,  $\text{CD}_3\text{OD}$ ): 5.34 (m, 1H, chol H-6), 4.30–3.40 (17H, gal. protons and  $6 \times \text{CH}_2\text{O}$ ), 3.20 (m, 1H, chol H-3), 2.96 (m, 1H, SCH-a), 2.88 (m, 1H, SCH-b), 2.41–0.67 (remaining chol protons) with 1.0 (s, 3H,  $\text{CH}_3$ -19), 0.91 (d, 3H,  $\text{CH}_3$ -21,  $J_{20,21} = 6.4$  Hz), 0.87 (d, 6H,  $\text{CH}_3$ -26 and

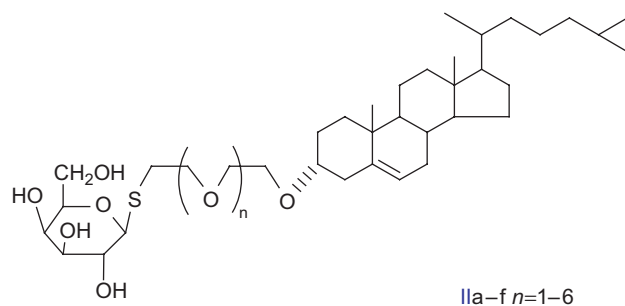
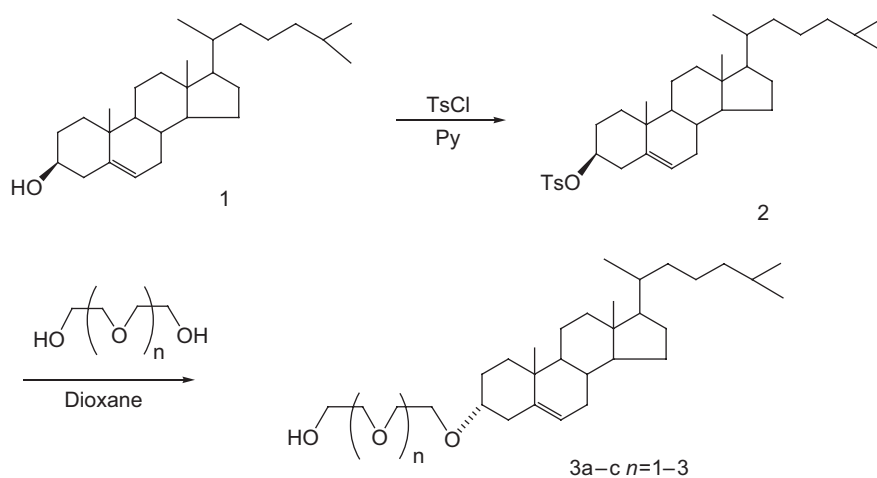
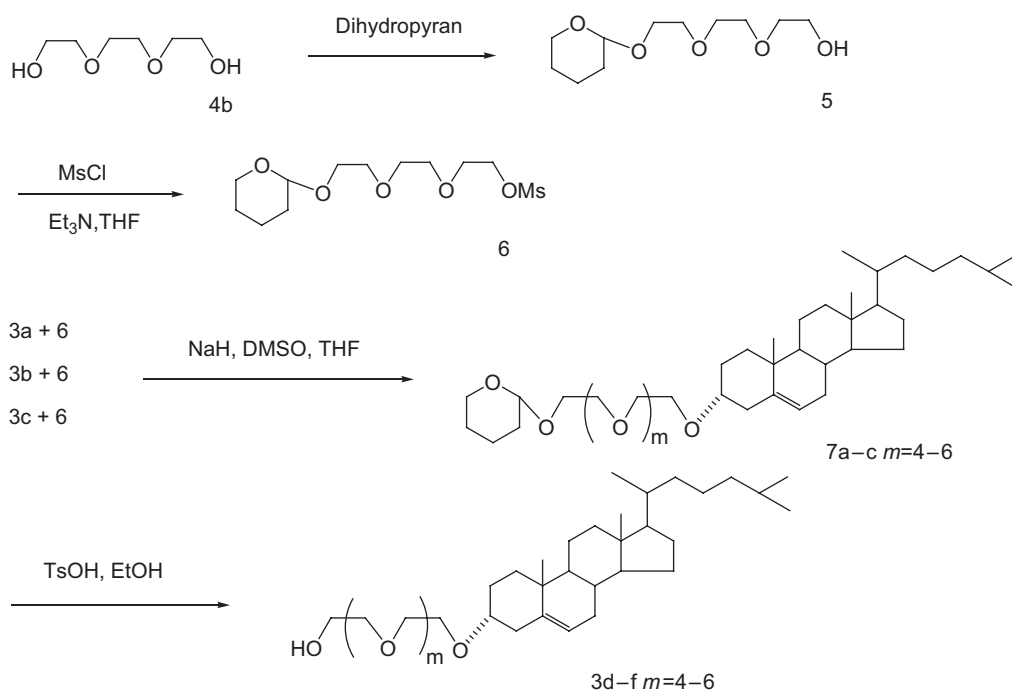


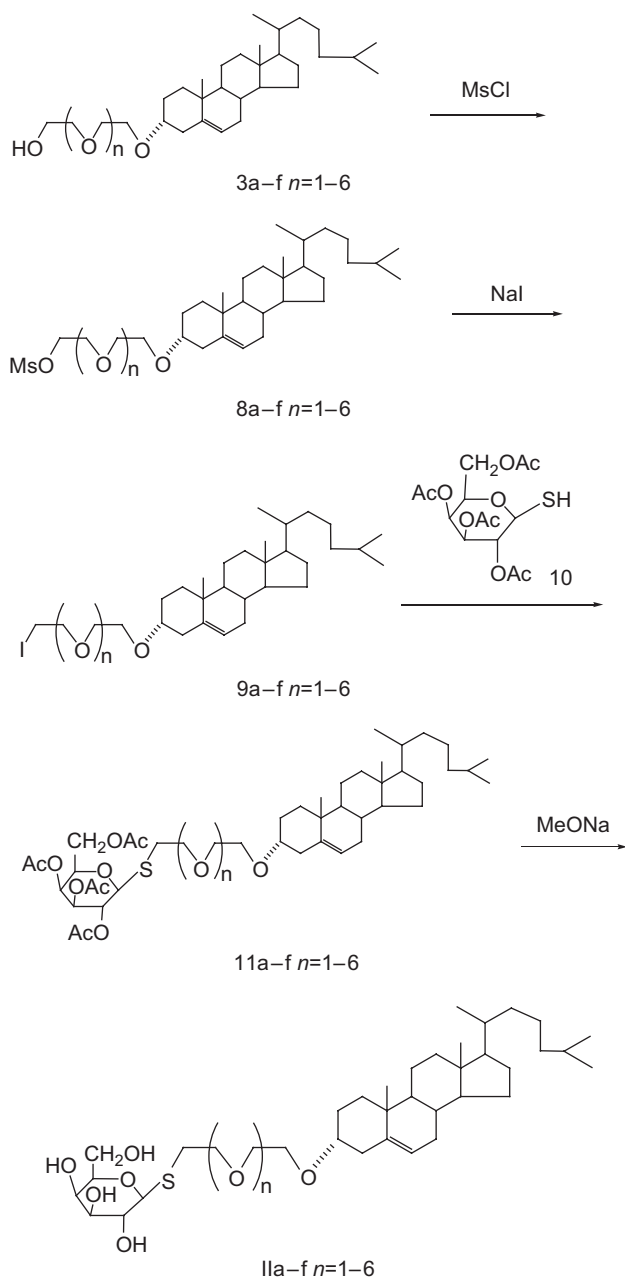
**Figure 1.** Structure of mono-antennary galactosides (target compound IIa-f).



**Scheme 1A.** The synthesis route of intermediate 3a-c.



**Scheme 1B.** The synthesis route of intermediate 3d-f.



**Scheme 1C.** The synthesis route of target compound IIa-f.

$\text{CH}_3$ -27,  $J_{25,26} = J_{25,27} = 6.8$  Hz), 0.67 (s, 3H,  $\text{CH}_3$ -18). MS ( $m/z$ ): ( $\text{M}+\text{Na}$ )<sup>+</sup> 719.

Compound IIc ( $\text{C}_{41}\text{H}_{72}\text{O}_9\text{S}$ ): <sup>1</sup>HNMR ( $\delta$  ppm, 400 MHz,  $\text{CD}_3\text{OD}$ ): 5.35 (m, 1H, chol H-6), 4.33–3.58 (21H, gal. protons and  $8 \times \text{CH}_2\text{O}$ ), 3.20 (m, 1H, chol H-3), 2.96 (m, 1H, SCH-a), 2.88 (m, 1H, SCH-b), 2.39–0.67 (remaining chol protons) with 1.0 (s, 3H,  $\text{CH}_3$ -19), 0.91 (d, 3H,  $\text{CH}_3$ -21,  $J_{20,21} = 6.0$  Hz), 0.86 (d, 6H,  $\text{CH}_3$ -26 and  $\text{CH}_3$ -27,  $J_{25,26} = J_{25,27} = 6.4$  Hz), 0.67 (s, 3H,  $\text{CH}_3$ -18). MS ( $m/z$ ): ( $\text{M}+\text{Na}$ )<sup>+</sup> 763.

Compound IId ( $\text{C}_{43}\text{H}_{76}\text{O}_{10}\text{S}$ ): <sup>1</sup>HNMR ( $\delta$  ppm, 400 MHz,  $\text{CD}_3\text{OD}$ ): 5.35 (m, 1H, chol H-6), 4.33–3.43 (25H, gal. protons and  $10 \times \text{CH}_2\text{O}$ ), 3.20 (m, 1H, chol H-3), 2.94 (m, 1H, SCH-a), 2.82 (m, 1H, SCH-b), 2.39–0.71

(remaining chol protons) with 1.01 (s, 3H,  $\text{CH}_3$ -19), 0.93 (d, 3H,  $\text{CH}_3$ -21,  $J_{20,21} = 6.8$  Hz), 0.87 (d, 6H,  $\text{CH}_3$ -26 and  $\text{CH}_3$ -27,  $J_{25,26} = J_{25,27} = 7.2$  Hz), 0.71 (s, 3H,  $\text{CH}_3$ -18). MS ( $m/z$ ): ( $\text{M}+\text{Na}$ )<sup>+</sup> 807.

Compound IIe ( $\text{C}_{45}\text{H}_{80}\text{O}_{11}\text{S}$ ): <sup>1</sup>HNMR ( $\delta$  ppm, 400 MHz,  $\text{CD}_3\text{OD}$ ): 5.35 (m, 1H, chol H-6), 4.33–3.43 (29H, gal. protons and  $12 \times \text{CH}_2\text{O}$ ), 3.20 (m, 1H, chol H-3), 2.94 (m, 1H, SCH-a), 2.82 (m, 1H, SCH-b), 2.39–0.71 (remaining chol protons) with 1.01 (s, 3H,  $\text{CH}_3$ -19), 0.93 (d, 3H,  $\text{CH}_3$ -21,  $J_{20,21} = 6.8$  Hz), 0.87 (d, 6H,  $\text{CH}_3$ -26 and  $\text{CH}_3$ -27,  $J_{25,26} = J_{25,27} = 6.4$  Hz), 0.71 (s, 3H,  $\text{CH}_3$ -18). MS ( $m/z$ ): ( $\text{M}+\text{Na}$ )<sup>+</sup> 851.

Compound IIIf ( $\text{C}_{47}\text{H}_{84}\text{O}_{12}\text{S}$ ): <sup>1</sup>HNMR ( $\delta$  ppm, 400 MHz,  $\text{CD}_3\text{OD}$ ): 5.35 (m, 1H, chol H-6), 4.33–3.58 (33H, gal. protons and  $14 \times \text{CH}_2\text{O}$ ), 3.20 (m, 1H, chol H-3), 2.94 (m, 1H, SCH-a), 2.82 (m, 1H, SCH-b), 2.39–0.71 (remaining chol protons) with 1.01 (s, 3H,  $\text{CH}_3$ -19), 0.93 (d, 3H,  $\text{CH}_3$ -21,  $J_{20,21} = 6.8$  Hz), 0.86 (d, 6H,  $\text{CH}_3$ -26 and  $\text{CH}_3$ -27,  $J_{25,26} = J_{25,27} = 6.4$  Hz), 0.71 (s, 3H,  $\text{CH}_3$ -18). MS ( $m/z$ ): ( $\text{M}+\text{Na}$ )<sup>+</sup> 895.

### Synthesis route of target compound IIIa-f (Figure 2, Scheme 2)

The compound 13 (Hukkamaki & Pakkanen, 2001) was prepared by the Michael addition reaction of pentaerythritol with acrylonitrile in the presence of sodium hydrochloride, which was converted into the compound 14 through ethanolysis. With the four ester functionalities reduced by  $\text{LiAlH}_4$ , the product tetra-(*o*-hydroxypropyloxymethyl) methane 15 (Newkome, Mishra, & Moorefield, 2002) was obtained, which was then methylsulfonylated, affording mesylate 16. Followed by coupling with 3a, the conjugate 17a was prepared and subsequently converted into iodide 18a by treating with NaI in refluxing butanone. Conjugation of 18a with 2,3,4,6-tetra-O-acetyl-1-thio- $\beta$ -D-galactopyranose resulted in the clustered trisaccharide derivative 19a. Then the target compound IIIa was obtained by deacetylation of 19a. Compound IIIa ( $\text{C}_{66}\text{H}_{118}\text{O}_{22}\text{S}_3$ ): <sup>1</sup>HNMR ( $\delta$  ppm, 400 MHz,  $\text{CD}_3\text{OD}$ ): 5.36 (m, 1H, chol H-6), 4.31 (d, 3H,  $3 \times$  gal.  $\text{H}_1$ ,  $J = 9.6$  Hz), 3.88 (d, 3H,  $3 \times$  gal.  $\text{H}_4$ ,  $J = 3.2$  Hz), 3.76–3.45 (m, 33H,  $3 \times$  gal.  $\text{H}_2, \text{H}_3, \text{H}_5, \text{H}_6, \text{H}_6'$  protons and  $9 \times \text{CH}_2\text{O}$ ), 3.37 (s, 8H,  $4 \times \text{CCH}_2\text{O}$ ), 3.19 (m, 1H, chol H-3), 2.78 (m, 6H, SCH-a, SCH-b), 2.35–0.72 (remaining chol protons,  $4 \times \text{CCH}_2\text{C}$ ) with 1.02 (s, 3H,  $\text{CH}_3$ -19), 0.91 (d, 3H,  $\text{CH}_3$ -21,  $J_{20,21} = 6.4$  Hz), 0.86 (d, 6H,  $\text{CH}_3$ -26 and  $\text{CH}_3$ -27,  $J_{25,26} = J_{25,27} = 6.4$  Hz), 0.72 (s, 3H,  $\text{CH}_3$ -18). MS ( $m/z$ ): ( $\text{M}+\text{Na}$ )<sup>+</sup> 1381.6.

The synthetic route of compound IIIb-f is similar to that of compound IIIa. Compound IIIb ( $\text{C}_{68}\text{H}_{122}\text{O}_{23}\text{S}_3$ ): <sup>1</sup>HNMR ( $\delta$  ppm, 400 MHz,  $\text{CD}_3\text{OD}$ ): 5.36 (m, 1H, chol H-6), 4.31 (d, 3H,  $3 \times$  gal.  $\text{H}_1$ ,  $J = 9.6$  Hz), 3.88 (d, 3H,  $3 \times$  gal.  $\text{H}_4$ ,  $J = 3.6$  Hz), 3.77–3.45 (m, 37H,  $3 \times$  gal.  $\text{H}_2, \text{H}_3, \text{H}_5, \text{H}_6, \text{H}_6'$  protons and  $11 \times \text{CH}_2\text{O}$ ), 3.37 (s, 8H,  $4 \times \text{CCH}_2\text{O}$ ), 3.19 (m, 1H, chol H-3), 2.79 (m, 6H, SCH-a, SCH-b), 2.37–0.71 (remaining chol protons,  $4 \times \text{CCH}_2\text{C}$ ) with 1.02 (s, 3H,  $\text{CH}_3$ -19), 0.91 (d, 3H,  $\text{CH}_3$ -21,  $J_{20,21} = 6.8$  Hz), 0.86 (d, 6H,  $\text{CH}_3$ -26 and



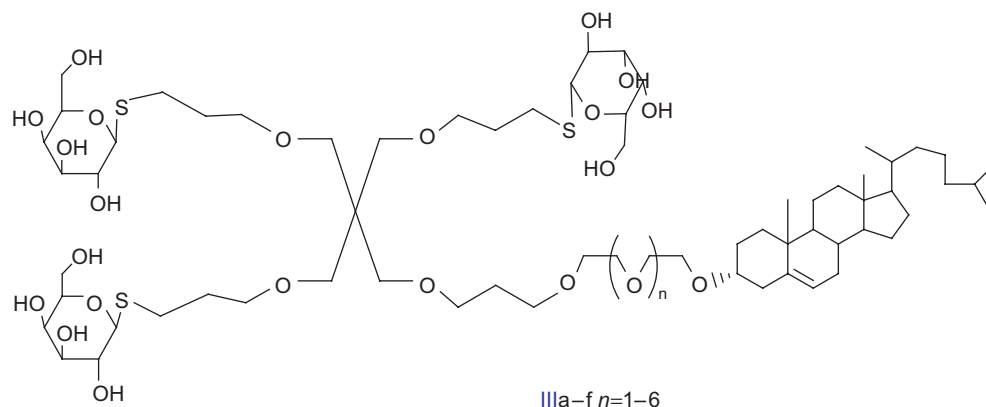


**Figure 2.** The structure of tri-antennary galactosides (target compound IIIa-f).

CH<sub>3</sub>-27,  $J_{25,26} = J_{25,27} = 6.4$  Hz), 0.71 (s, 3H, CH<sub>3</sub>-18). MS ( $m/z$ ): (M+Na)<sup>+</sup> 1426.2.

Compound IIIc (C<sub>70</sub>H<sub>126</sub>O<sub>24</sub>S<sub>3</sub>): <sup>1</sup>HNMR ( $\delta$  ppm, 400 MHz, CD<sub>3</sub>OD): 5.36 (m, 1H, chol H-6), 4.30 (d, 3H, 3  $\times$  gal. H<sub>1</sub>,  $J = 9.2$  Hz), 3.88 (d, 3H, 3  $\times$  gal. H<sub>4</sub>,  $J = 3.6$  Hz), 3.75-3.43 (m, 41H, 3  $\times$  gal. H<sub>2</sub>, H<sub>3</sub>, H<sub>5</sub>, H<sub>6</sub>, H<sub>6'</sub> protons and 13  $\times$  CH<sub>2</sub>O), 3.36 (s, 8H, 4  $\times$  CCH<sub>2</sub>O), 3.18 (m, 1H, chol H-3), 2.79 (m, 6H, SCH-a, SCH-b), 2.37-0.71 (remaining chol protons, 4  $\times$  CCH<sub>2</sub>C) with 1.02 (s, 3H, CH<sub>3</sub>-19), 0.91 (d, 3H, CH<sub>3</sub>-21,  $J_{20,21} = 6.4$  Hz), 0.86 (d, 6H, CH<sub>3</sub>-26 and CH<sub>3</sub>-27,  $J_{25,26} = J_{25,27} = 6.4$  Hz), 0.71 (s, 3H, CH<sub>3</sub>-18). MS ( $m/z$ ): (M+Na)<sup>+</sup> 1469.9.

Compound IIIId (C<sub>72</sub>H<sub>130</sub>O<sub>25</sub>S<sub>3</sub>): <sup>1</sup>HNMR ( $\delta$  ppm, 400 MHz, CD<sub>3</sub>OD): 5.35 (m, 1H, chol H-6), 4.31 (d, 3H, 3  $\times$  gal. H<sub>1</sub>,  $J = 9.2$  Hz), 3.88 (d, 3H, 3  $\times$  gal. H<sub>4</sub>,  $J = 3.6$  Hz), 3.78-3.43 (m, 45H, 3  $\times$  gal. H<sub>2</sub>, H<sub>3</sub>, H<sub>5</sub>, H<sub>6</sub>, H<sub>6'</sub> protons and 15  $\times$  CH<sub>2</sub>O), 3.34 (s, 8H, 4  $\times$  CCH<sub>2</sub>O), 3.18 (m, 1H, chol H-3), 2.78 (m, 6H, SCH-a, SCH-b), 2.37-0.70 (remaining chol protons, 4  $\times$  CCH<sub>2</sub>C) with 1.02 (s, 3H, CH<sub>3</sub>-19), 0.91 (d, 3H, CH<sub>3</sub>-21,  $J_{20,21} = 6.4$  Hz), 0.86 (d, 6H, CH<sub>3</sub>-26 and CH<sub>3</sub>-27,  $J_{25,26} = J_{25,27} = 6.4$  Hz), 0.70 (s, 3H, CH<sub>3</sub>-18). MS ( $m/z$ ): (M+Na)<sup>+</sup> 1514.1.

Compound IIIe (C<sub>74</sub>H<sub>134</sub>O<sub>26</sub>S<sub>3</sub>): <sup>1</sup>HNMR ( $\delta$  ppm, 400 MHz, CD<sub>3</sub>OD): 5.35 (m, 1H, chol H-6), 4.31 (d, 3H, 3  $\times$  gal. H<sub>1</sub>,  $J = 9.8$  Hz), 3.88 (d, 3H, 3  $\times$  gal. H<sub>4</sub>,  $J = 3.2$  Hz), 3.77-3.43 (m, 49H, 3  $\times$  gal. H<sub>2</sub>, H<sub>3</sub>, H<sub>5</sub>, H<sub>6</sub>, H<sub>6'</sub> protons and 17  $\times$  CH<sub>2</sub>O), 3.34 (s, 8H, 4  $\times$  CCH<sub>2</sub>O), 3.18 (m, 1H, chol H-3), 2.78 (m, 6H, SCH-a, SCH-b), 2.37-0.70 (remaining chol protons, 4  $\times$  CCH<sub>2</sub>C) with 1.02 (s, 3H, CH<sub>3</sub>-19), 0.91 (d, 3H, CH<sub>3</sub>-21,  $J_{20,21} = 6.4$  Hz), 0.86 (d, 6H, CH<sub>3</sub>-26 and CH<sub>3</sub>-27,  $J_{25,26} = J_{25,27} = 6.4$  Hz), 0.70 (s, 3H, CH<sub>3</sub>-18). MS ( $m/z$ ): (M+Na)<sup>+</sup> 1557.9.

Compound IIIf (C<sub>76</sub>H<sub>138</sub>O<sub>27</sub>S<sub>3</sub>): <sup>1</sup>HNMR ( $\delta$  ppm, 400 MHz, CD<sub>3</sub>OD): 5.35 (m, 1H, chol H-6), 4.31 (d, 3H, 3  $\times$  gal. H<sub>1</sub>,  $J = 9.8$  Hz), 3.88 (d, 3H, 3  $\times$  gal. H<sub>4</sub>,  $J = 3.2$  Hz), 3.77-3.43 (m, 53H, 3  $\times$  gal. H<sub>2</sub>, H<sub>3</sub>, H<sub>5</sub>, H<sub>6</sub>, H<sub>6'</sub> protons and 19  $\times$  CH<sub>2</sub>O), 3.34 (s, 8H, 4  $\times$  CCH<sub>2</sub>O), 3.18 (m, 1H, chol H-3), 2.78 (m, 6H, SCH-a, SCH-b), 2.37-0.71 (remaining chol protons, 4  $\times$  CCH<sub>2</sub>C) with 1.02 (s, 3H, CH<sub>3</sub>-19), 0.91 (d, 3H, CH<sub>3</sub>-21,  $J_{20,21} = 6.4$  Hz), 0.87 (d, 6H, CH<sub>3</sub>-26 and CH<sub>3</sub>-27,  $J_{25,26} = J_{25,27} = 6.8$  Hz), 0.71 (s, 3H, CH<sub>3</sub>-18). MS ( $m/z$ ): (M+Na)<sup>+</sup> 1601.9.

### Synthesis route of target compound IVa-f (Figure 3, Scheme 3B)

The sexi-( $\beta$ -cyanoethyl) cyclohexanehexo-lether 21 could be afforded by Michael reaction of cyclohexanehexol with acrylonitrile, followed by ethanolysis, resulting in the sexi-( $\beta$ -carboethoxyethyl) cyclohexanehexo-lether 22. The reduction of four ester functionalities of 22 was achieved under anhydrous condition, yielding the hexa-antennary alcohol 23, which was subsequently methylsulfonylated to the intermediate 24 (Scheme 3A). By coupling with 3a, 25a was obtained and could be converted into iodide 26a by treating with NaI in refluxing butanone. Using 2,3,4,6-tetra-*O*-acetyl-1-thio- $\beta$ -D-galactopyranose as glycosyl donor, the clustered penta-saccharide derivative 27a was synthesized, the deacetylation of which yielded the desired product IVa (C<sub>85</sub>H<sub>150</sub>O<sub>34</sub>S<sub>5</sub>). <sup>1</sup>HNMR ( $\delta$  ppm, 400 MHz, CD<sub>3</sub>OD): 5.37 (m, 1H, chol H-6), 4.34 (t, 5H, 5  $\times$  gal. H<sub>1</sub>,  $J = 9.6$  Hz), 3.93-3.43 (m, 56H, 5  $\times$  gal. H<sub>2</sub>, H<sub>3</sub>, H<sub>4</sub>, H<sub>5</sub>, H<sub>6</sub>, H<sub>6'</sub> protons and 6  $\times$  CHOCH<sub>2</sub>, 2  $\times$  OCH<sub>2</sub>CH<sub>2</sub>O), 3.19 (m, 1H, chol H-3), 2.89-2.81 (m, 10H, SCH-a, SCH-b), 2.40-0.71 (remaining chol protons, 6  $\times$  CCH<sub>2</sub>C) with 1.02 (s, 3H, CH<sub>3</sub>-19), 0.93 (d, 3H, CH<sub>3</sub>-21,  $J_{20,21} = 6.4$  Hz), 0.87 (d, 6H, CH<sub>3</sub>-26 and CH<sub>3</sub>-27,  $J_{25,26} = J_{25,27} = 6.4$  Hz), 0.71 (s, 3H, CH<sub>3</sub>-18). MS ( $m/z$ ): (M+Na)<sup>+</sup> 1898.1.

*The synthetic route of compound IVb-f is similar to that of compound IVa.* Compound IVb (C<sub>87</sub>H<sub>154</sub>O<sub>35</sub>S<sub>5</sub>): <sup>1</sup>HNMR ( $\delta$  ppm, 400 MHz, CD<sub>3</sub>OD): 5.36 (m, 1H, chol H-6), 4.34 (m, 5H, 5  $\times$  gal. H<sub>1</sub>), 3.95-3.43 (m, 60H, 5  $\times$  gal. H<sub>2</sub>, H<sub>3</sub>, H<sub>4</sub>, H<sub>5</sub>, H<sub>6</sub>, H<sub>6'</sub> protons and 6  $\times$  CHOCH<sub>2</sub>, 3  $\times$  OCH<sub>2</sub>CH<sub>2</sub>O), 3.18 (m, 1H, chol H-3), 2.90-2.81 (m, 10H, SCH-a, SCH-b), 2.39-0.71 (remaining chol protons, 6  $\times$  CCH<sub>2</sub>C) with 1.02 (s, 3H, CH<sub>3</sub>-19), 0.93 (d, 3H, CH<sub>3</sub>-21,  $J_{20,21} = 6.8$  Hz), 0.87 (d, 6H, CH<sub>3</sub>-26 and CH<sub>3</sub>-27,  $J_{25,26} = J_{25,27} = 6.4$  Hz), 0.71 (s, 3H, CH<sub>3</sub>-18). MS ( $m/z$ ): (M+Na)<sup>+</sup> 1941.9.

Compound IVc (C<sub>89</sub>H<sub>158</sub>O<sub>36</sub>S<sub>5</sub>): <sup>1</sup>HNMR ( $\delta$  ppm, 400 MHz, CD<sub>3</sub>OD): 5.35 (m, 1H, chol H-6), 4.34 (m, 5H, 5  $\times$  gal. H<sub>1</sub>), 3.93-3.43 (m, 64H, 5  $\times$  gal. H<sub>2</sub>, H<sub>3</sub>, H<sub>4</sub>, H<sub>5</sub>, H<sub>6</sub>, H<sub>6'</sub> protons and 6  $\times$  CHOCH<sub>2</sub>, 4  $\times$  OCH<sub>2</sub>CH<sub>2</sub>O), 3.19 (m, 1H, chol H-3), 2.89-2.81 (m, 10H, SCH-a, SCH-b), 2.40-0.71 (remaining chol protons, 6  $\times$  CCH<sub>2</sub>C) with 1.01 (s, 3H,

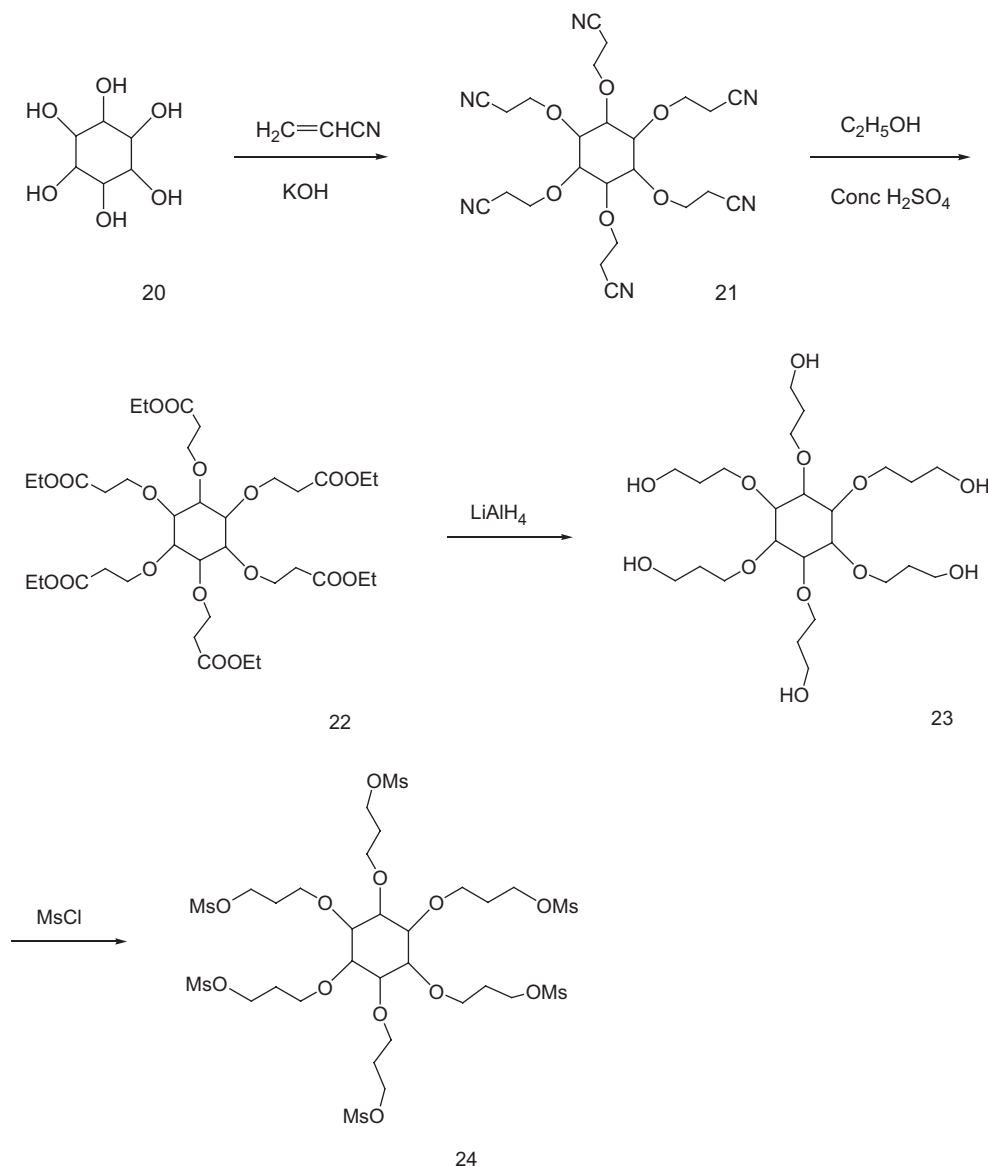
CH<sub>3</sub>-19), 0.93(d, 3H, CH<sub>3</sub>-21,  $J_{20,21}$  = 6.4 Hz), 0.87 (d, 6H, CH<sub>3</sub>-26 and CH<sub>3</sub>-27,  $J_{25,26}$  =  $J_{25,27}$  = 6.4 Hz), 0.71 (s, 3H, CH<sub>3</sub>-18). MS ( $m/z$ ): (M+Na)<sup>+</sup> 1985.9.

Compound IVd (C<sub>91</sub>H<sub>162</sub>O<sub>37</sub>S<sub>5</sub>): 5.34 (m, 1H, chol H-6), 4.33(m, 5H, 5 × gal. H<sub>1</sub>), 3.91–3.43 (m, 68H, 5 × gal. H<sub>2</sub>, H<sub>3</sub>, H<sub>4</sub>, H<sub>5</sub>, H<sub>6</sub>, H<sub>6'</sub> protons and 6 × CHOCH<sub>2</sub>, 5 × OCH<sub>2</sub>CH<sub>2</sub>O), 3.18 (m, 1H, chol H-3), 2.89–2.81 (m, 10H, SCH-a, SCH-b), 2.40–0.71 (remaining chol protons, 6 × CCH<sub>2</sub>C) with 1.01 (s, 3H, CH<sub>3</sub>-19), 0.93 (d, 3H, CH<sub>3</sub>-21,  $J_{20,21}$  = 6.4 Hz), 0.87 (d, 6H, CH<sub>3</sub>-26 and CH<sub>3</sub>-27,  $J_{25,26}$  =  $J_{25,27}$  = 6.4 Hz), 0.71 (s, 3H, CH<sub>3</sub>-18). MS ( $m/z$ ): (M+Na)<sup>+</sup> 2029.9.

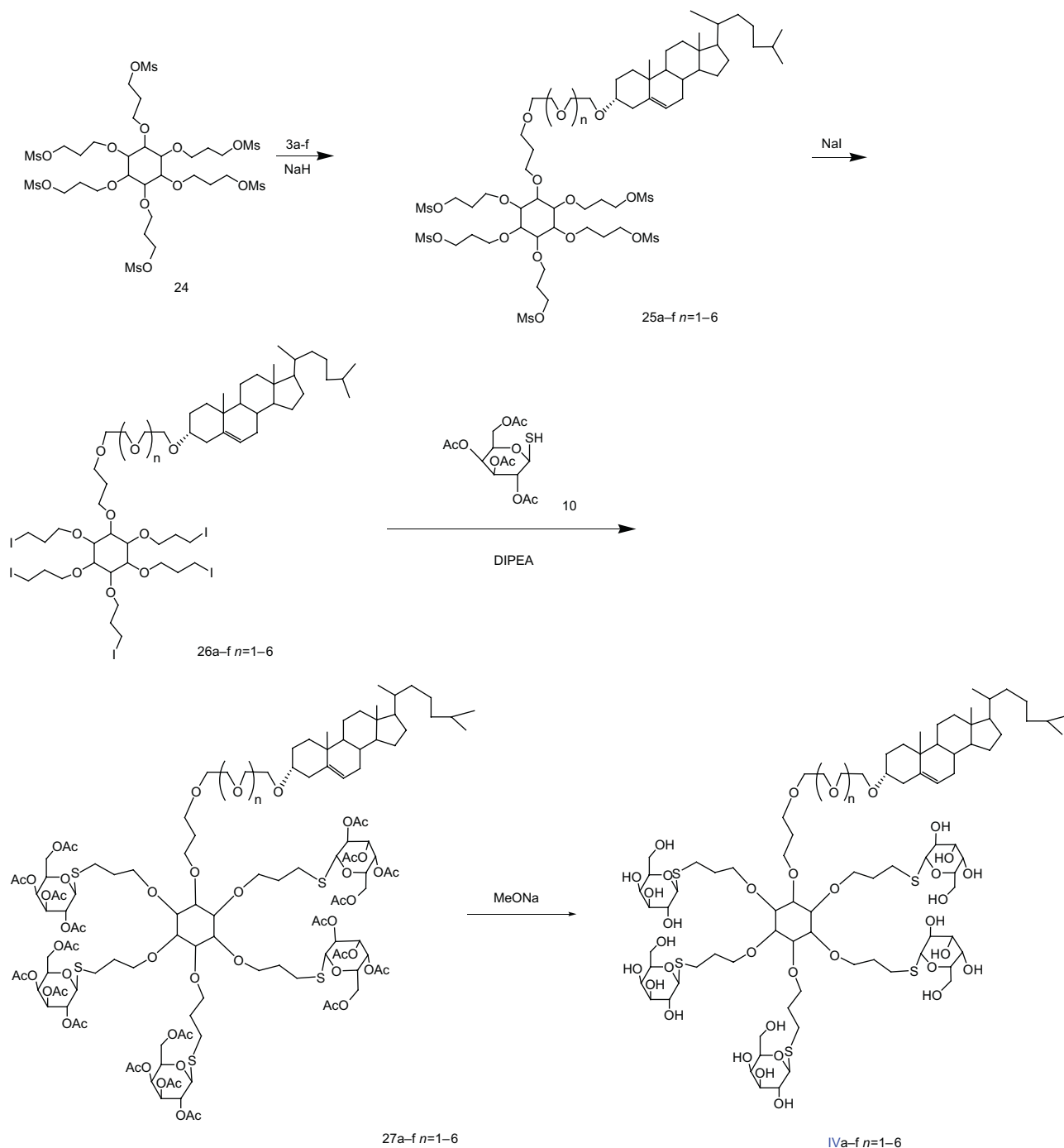
Compound IVe (C<sub>93</sub>H<sub>166</sub>O<sub>38</sub>S<sub>5</sub>): <sup>1</sup>HNMR (δ ppm, 400 MHz, CD<sub>3</sub>OD): 5.35 (m, 1H, chol H-6), 4.34 (m, 5H, 5 × gal. H<sub>1</sub>), 3.93–3.43 (m, 72H, 5 × gal. H<sub>2</sub>, H<sub>3</sub>, H<sub>4</sub>, H<sub>5</sub>, H<sub>6</sub>, H<sub>6'</sub> protons and 6 × CHOCH<sub>2</sub>, 6 × OCH<sub>2</sub>CH<sub>2</sub>O), 3.18 (m, 1H,

chol H-3), 2.89–2.81 (m, 10H, SCH-a, SCH-b), 2.40–0.70 (remaining chol protons, 6 × CCH<sub>2</sub>C) with 1.01 (s, 3H, CH<sub>3</sub>-19), 0.93(d, 3H, CH<sub>3</sub>-21,  $J_{20,21}$  = 6.4 Hz), 0.87 (d, 6H, CH<sub>3</sub>-26 and CH<sub>3</sub>-27,  $J_{25,26}$  =  $J_{25,27}$  = 6.4 Hz), 0.70 (s, 3H, CH<sub>3</sub>-18). MS ( $m/z$ ): (M+Na)<sup>+</sup> 2073.8.

Compound IVf (C<sub>95</sub>H<sub>170</sub>O<sub>42</sub>S<sub>5</sub>): <sup>1</sup>HNMR (δ ppm, 400 MHz, CD<sub>3</sub>OD): 5.36 (m, 1H, chol H-6), 4.34 (m, 5H, 5 × gal. H<sub>1</sub>), 3.93–3.43 (m, 76H, 5 × gal. H<sub>2</sub>, H<sub>3</sub>, H<sub>4</sub>, H<sub>5</sub>, H<sub>6</sub>, H<sub>6'</sub> protons and 6 × CHOCH<sub>2</sub>, 7 × OCH<sub>2</sub>CH<sub>2</sub>O), 3.19 (m, 1H, chol H-3), 2.89–2.81 (m, 10H, SCH-a, SCH-b), 2.40–0.71 (remaining chol protons, 6 × CCH<sub>2</sub>C) with 1.02 (s, 3H, CH<sub>3</sub>-19), 0.93(d, 3H, CH<sub>3</sub>-21,  $J_{20,21}$  = 6.4 Hz), 0.87 (d, 6H, CH<sub>3</sub>-26 and CH<sub>3</sub>-27,  $J_{25,26}$  =  $J_{25,27}$  = 6.4 Hz), 0.71 (s, 3H, CH<sub>3</sub>-18). MS ( $m/z$ ): (M+Na)<sup>+</sup> 2117.6.



Scheme 3A. The synthesis route of intermediate compound 24.



**Scheme 3B.** Synthesis route of target compound IVa-f.

### Plasmid DNA preparation

The plasmid pORF lacZ (3.54kb) is a eukaryotic expression vector which contains the EF-1a/HTLV hybrid promoter within an intron. The lacZ gene codes for the enzyme  $\beta$ -galactosidase, whose activity allows for the quick determination of cells expressing the lacZ gene. pORF-lacZ plasmid DNA was isolated and purified from DH5 $\alpha$  E. coli using the Qiagen Giga Endo-free plasmid purification kit. DNA concentration and purity were

quantified by UV absorbance at 260 and 280 nm on a GBC UV cintra 10e Spectrophotometer. The structural integrity and topology of purified DNA was analyzed by agarose gel electrophoresis.

### LPD preparation

A control cationic liposome was composed of DDAB, DOPE and cholesterol at a molar ratio of 3:1:1. By contrast, Gal-liposomes, specifically, Liposome Iia-f, Liposome

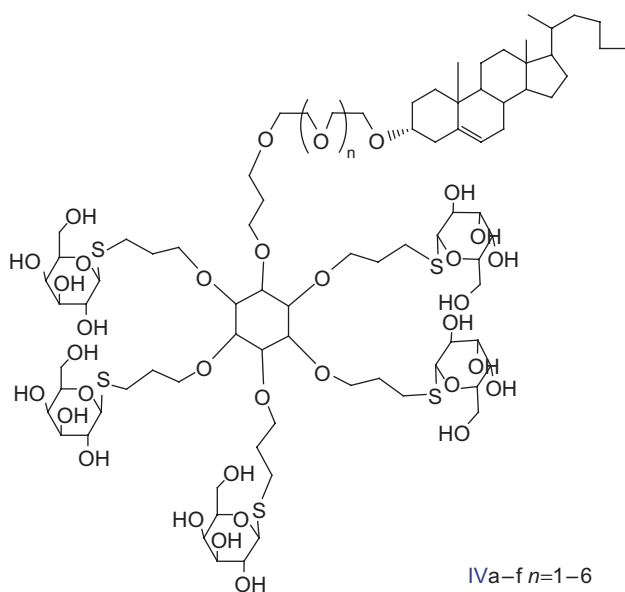


**Figure 3.** Structure of penta-antennary galactosides (target compound IVa-f).

IIIa-f, and Liposome IVa-f, consisted of DDAB, DOPE, and cholesterylated galactosides with different amount of galactose residues and various spacer lengths, at a molar ratio of 3:1:1. The lipid mixture was dissolved in appropriate chloroform and a thin lipid film was formed in a round-bottomed flask by drying the solvent under a stream of nitrogen gas. Residual chloroform was further removed by placing the flask in a desiccator vacuum for 30 min. The film was hydrated with the addition of 5% dextrose. Then the lipid suspension was ultrasounded by ultrasonic probe.

LPDs were prepared as described previously (Sun et al., 2005). To form protamine/DNA polycation, the protamine/DNA ratio was used 1.5:1. In brief, DNA and protamine were both diluted with 5% dextrose to get stock concentrations of 500  $\mu\text{g}/\text{mL}$  and 150  $\mu\text{g}/\text{mL}$ , respectively. Appropriate amount of DNA stock solution was added dropwise to a certain amount of protamine stock solution with mild stirring. After mixing, the resulted polyplexes (DNA-polycation complexes) were incubated for 10 min at room temperature. Preformed cationic liposomes were subsequently added to the DNA/protamine polyplexes under mild vortexing to achieve the desired final component concentrations and ratios. Thus, the nongalactosylated formulation LPD0 was obtained by mixing the polyplexes and the control cationic liposome mentioned above while the galactosylated formulations LPDIIa-f, LPDIIIa-f, and LPDIVa-f were prepared by mixing the polyplexes and Gal-liposomes consisting of DDAB, DOPE and corresponding cholesterylated galactosides at a molar ratio of 3:1:1.

### Electron microscopy

LPD0 and Gal-LPD were examined by transmission electron microscopy (JEM-100SX, Japan). Samples were prepared by placing a drop of LPD suspension onto a copper grid and air-drying, followed by negative staining with a drop of 2% aqueous solution of uranyl acetate for contrast enhancement. The air dried samples were then directly examined under the transmission microscope.

### Size and zeta potential

Diameter and surface charge of DNA polyplexes, the control cationic liposome LPD0 and LPDs were measured by photon correlation spectroscopy (PCS) (Zetasizer Nano ZS90, Malvern instruments Ltd., UK) with a 50 mV laser. A measure of 20 mL of LPD was diluted by 2 mL of 5% dextrose and added into the sample cell. The measurement time was set to 2 min (rapid measurement) and each run consisted of 10 subruns. The measurements were done at 25°C at an angle of 90°C. The size distribution follows a lognormal distribution. The potential of the lipid carriers at the surface of spheres, called the zeta potential, which was derived from mobility of particles in electric field by applying the smoluchowsky relationship, was measured at least three times at appropriate concentrations of samples.

### Protection assay of DNA

Briefly, 4  $\mu\text{L}$  of DNase I (2 units) or PBS in DNase digestion buffer (50 mmol, Tris-Cl, pH 7.6 and 10 mmol  $\text{MgCl}_2$ ) was added to 4  $\mu\text{g}$  of naked plasmid DNA or LPDs, and incubated at 37°C for different time periods. For DNase inactivation, all samples were treated with EDTA (0.5 mol). Then Triton X-100 was mixed with each sample to destroy the lipolayers. After 2 min' brief shaking, heparin solution was added to the mixture at a final concentration of 0.9% (w/v). The final samples were incubated for 2 h and electrophoresis was performed with 1.0% agarose gel in TAE running buffer for 2 h at 80 V. Images were analyzed using Kodak Digital Science 1D software to obtain in the form of volume per area.

### Cell transfection

HepG2 and A549 cells were cultured in RPMI-1640 with 10% fetal bovine serum and streptomycin (100 mg/mL). The cells were seeded at  $2 \times 10^5$  cells/well onto 12-well plates 24 h before transfection so that they would be 70% confluence at the time of transfection. After the cells were washed twice by PBS, 0.5 mL of serum-free, antibiotics-free medium were added into each well. For each well, LPD containing 4  $\mu\text{g}$  (if not mentioned specifically) of pORF-1acZ was diluted to 0.5 mL by the serum-free

medium, and then gently overlaid onto the cells. The cells were incubated with LPD for 5 h at 37°C in a CO<sub>2</sub> incubator. Following incubation, LPD was removed and the cell surfaces were rinsed thoroughly and treated with 2 mL fresh complete medium. Then the cells were returned to the incubator for a further 45 h to allow intracellular gene expression to proceed. As a control, the commercial transfection reagent Lipofectamine™ 2000 was used to transfect cells according to manufacturer's instructions.

### ***β-Galactosidase assay***

Expression of  $\beta$ -galactosidase genes was measured with  $\beta$ -gal assay kit according to the manufacturer's instruction. The transfected HepG2 cells were washed once with PBS and lysed with lysis buffer (30 mL/well). Cell debris was removed by centrifugation at 12,000 g and 10 mL of the supernatant added to 50 mL of cleavage buffer containing  $\beta$ -mercaptoethanol and 17 mL of ONPG solution. After incubation for 30 min at 37°C, the absorbance at 415 nm was measured. The total protein concentrations in cell lysates were determined using BCA assay (Pierce Chemical).

### ***Cytotoxicity assay***

Cytotoxicity of LPDs was studied using a colorimetric MTT assay. Briefly, cells were collected, counted and seeded in growth medium (200  $\mu$ L) into 96-well plates at a density of 15,000 cells/well. One day later, the cells were transfected as described above. After incubation for 45 h, 20  $\mu$ L of MTT (5 mg/mL) solution was added into each well and was allowed to react for 4 h at 37°C. Then the medium of each well was replaced with 150  $\mu$ L of DMSO and the plate was incubated for 10 min at room temperature. Absorbance at 570 nm was measured with an ELISA plate reader (Bio-Rad, Microplate Reader 550).

### ***Competitive inhibition assay of galactose***

HepG2 cells were cultured in RPMI-1640 with 10% fetal bovine serum and streptomycin (100 mg/mL). The cells were seeded at  $2 \times 10^5$  cells/well onto 12-well plates 24 h before transfection, so that they would be 70% confluence at the time of transfection. After the cells were washed twice by PBS, 0.5 mL serum-free, antibiotics-free medium were added into each well. For each well, LPD containing 4  $\mu$ g pORF-1acZ, LPD/80 mM D-galactose or LPD/80 mM D-mannose were diluted to 0.5 mL by the serum-free medium, and then gently overlaid onto the cells. Other steps were performed as previously mentioned in the cell transfection study and the transfection efficiency was measured.

## **Results**

### ***LPD characterization***

To prepare stable liposomes with high transfect efficiency, liposomes consisting of DDAB, DOPE, and cholesterol as well as protamine-DNA complexes protamine at different ratios were formulated. The protamine/DNA and the DDAB/DOPE/cholesterol ratio were optimized at 1.5 and 3:1:1, respectively, considering their size, zeta potential and transfect efficiency (Data not shown). Besides, we investigated the influence of the DDAB/DNA ratio on the particle size and zeta potential, as well as examined the *in vitro* transfect activity of LPD0, LPDIIb, LPDIIIc, and LPDIVE composing of different DDAB/DNA ratios. As shown in Table 1, for LPDs with the same DDAB/DNA ratio, the zeta potential decreased generally when cholesterylated thiogalactosides containing more galactosidase residues were incorporated into the structure. Also, it is notable that for LPD0 and LPDIIb groups, when the DDAB/DNA ratio was 2, the gene transfer ability was superior in HepG2 cells. However, for LPDIIIc and LPDIVE groups, though the transfect efficiency was not the highest with a DDAB/DNA ratio of 2, there was not significant difference ( $P > 0.05$ ) compared with the highest within each group. Therefore, considering the possible negative effects of DDAB on cell viability, the DDAB/DNA ratio was fixed at 2 in the following study.

LPD0 (without galactosylated cholesterols) and Gal-LPDs (LPDIIa-f, LPDIIIa-f, and LPDIVa-f) were prepared by adding cationic liposomes to protamine-DNA complexes. In general, zeta potential and particle size of LPDs were measured to between 19–57 mV and 107–221 nm, respectively (data not shown). Based on electron microscopy, the structure and morphology of the resulting LPD0 was described. As shown in Figure 4, the LPD0 particles and Gal-LPD particles (LPDIVE) were all nearly round-shaped, indicating the addition of galactose residues did not significantly change the shape of LPD while bringing an increase in particle size.

The DNA in the gene vehicle should be protected from degradation by DNase in the extracellular environment. Therefore, DNA protection assay was performed. As shown in Figure 5, after incubation with DNase I, naked plasmid DNA were completely digested within 5 min (lane 2). In contrast, the plasmid DNA incorporated in LPD still remained their integrity in supercoiled forms after incubation with DNase for 5 min and 2 h (lanes 3 and 4), suggesting its capability to be a potential gene vector.

### ***Cell transfection studies***

The modified LPDs containing the synthesized ligands were examined for their transfection efficiency. Two

**Table 1.** The influence of DDAB/DNA ratios on zeta potential, particle size, and  $\beta$ -galactosidase activity in HepG2 cells for LPD0, LPDIIf, LPDIIIc and LPDIVE. The DDAB, DOPE, and cholesterol was fixed at 1.5 and 3: 1: 1, respectively. The data points represent the mean $\pm$ SD of three experiments.

LPD	DDAB/DNA (w/w)	Zeta potential (mV)	Particle size (nm)	$\beta$ -Galactosidase activity (mU/mg protein)
LPD0	2	33.6 $\pm$ 1.8	109 $\pm$ 8.5	22.01 $\pm$ 1.98
	4	49.7 $\pm$ 3.8	107 $\pm$ 10.2	18.60 $\pm$ 2.35
	6	58.9 $\pm$ 4.0	110 $\pm$ 5.3	15.97 $\pm$ 2.61
	8	56.8 $\pm$ 3.2	115 $\pm$ 7.8	14.28 $\pm$ 3.67
LPD IIb	2	29.0 $\pm$ 2.7	112 $\pm$ 13.2	35.43 $\pm$ 3.25
	4	48.5 $\pm$ 3.5	109 $\pm$ 18.0	28.60 $\pm$ 3.41
	6	55.9 $\pm$ 3.4	107 $\pm$ 15.8	18.50 $\pm$ 3.52
	8	52.2 $\pm$ 5.2	112 $\pm$ 16.5	11.50 $\pm$ 2.17
LPD IIIc	2	19.4 $\pm$ 2.5	134 $\pm$ 12.8	39.79 $\pm$ 4.49
	4	22.0 $\pm$ 2.2	125 $\pm$ 21.6	43.21 $\pm$ 5.20
	6	26.2 $\pm$ 4.8	109 $\pm$ 10.5	38.33 $\pm$ 2.86
	8	34.5 $\pm$ 2.9	109 $\pm$ 15.9	15.77 $\pm$ 2.88
LPD IVe	2	20.3 $\pm$ 2.6	221 $\pm$ 14.7	47.20 $\pm$ 6.28
	4	21.8 $\pm$ 3.7	208 $\pm$ 12.8	50.21 $\pm$ 3.47
	6	27.8 $\pm$ 3.5	194 $\pm$ 23.1	52.26 $\pm$ 4.38
	8	32.6 $\pm$ 4.6	193 $\pm$ 21.5	30.75 $\pm$ 3.69

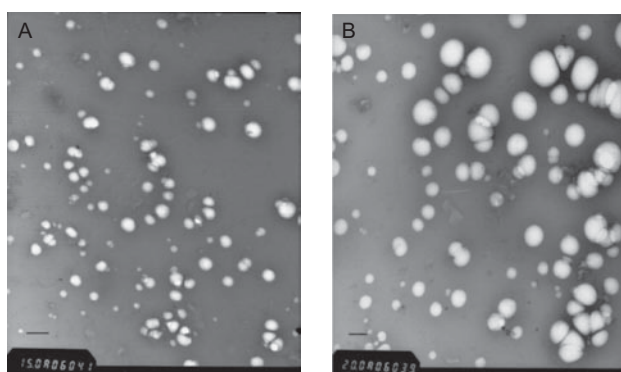


**Figure 4.** Transmission electronic micrographs of (A) LPD0, bar 200 nm, (B) LPDIVE, bar 200 nm. The nongalactosylated formulation LPD0 was obtained by mixing the DNA-protamine polyplex and the control cationic liposome and LPDIVE (Gal-LPD) was prepared by mixing the polyplex and Gal-liposome (DDAB/DOPE/cholesterylated galactosides 3:1:1). Then they were examined by transmission electron microscopy (JEM-100SX, Japan).

different cell lines were used: HepG2 cells derived from a human hepatocellular carcinoma expressing the ASGP-R (Schwartz et al., 1981), and the human alveolar epithelial cell line A549, which lacks the receptor (Nikken et al., 2009). The transfection efficacy of LPDs in gene delivery to HepG2 and A549 cells was studied to identify the receptor-mediated internalization. As indicated in Figure 7, compared with LPD0 which did not contain galactose residues, LPDIIa, LPDIIb, LPDIIIb, LPDIIIc, and LPDIVE-d-f has improved transfection efficiency in HepG2 cells. Also, it is notable that LPDIIb, LPDIIIc and LPDIVE, which possessed the most superior transfection efficiency among each galactosylated LPD group with the same spacer length, showed significant higher transfection efficiency than the commercial

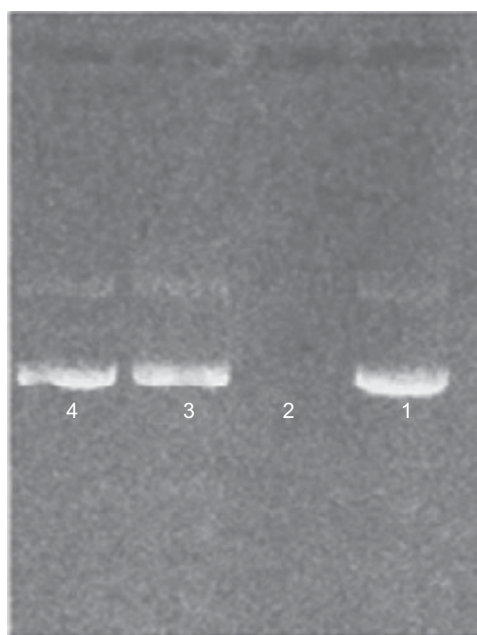


**Figure 5.** DNA protection assay by agarose gel electrophoresis of naked DNA and LPD subjected to DNase degradation. Lane 1: Naked DNA. Lane 2: Naked DNA incubated with DNase 5 min. Lane 3: LPD incubates with DNase 5 min. Lane 4: LPD incubates with DNase 2 h.

transfect reagent Lipofectamine<sup>TM</sup> 2000 ( $P < 0.05$ ) In contrast, all the LPDs containing cholesterylated thiogalactosides did not increase the transfection efficiency in A549 cells compared with LPD0. Instead, their transfection efficiency was significantly decreased in contrast to LPD0 ( $P < 0.05$ ) except LPDIIIc in A549 cells (Figure 6). Besides, it is worth mentioning that those Gal-LPDs, including LPDIIc-f, LPDIIIa, LPDIII-d-f, LPDIVE-a-c, did not significantly improve the transfection efficiency

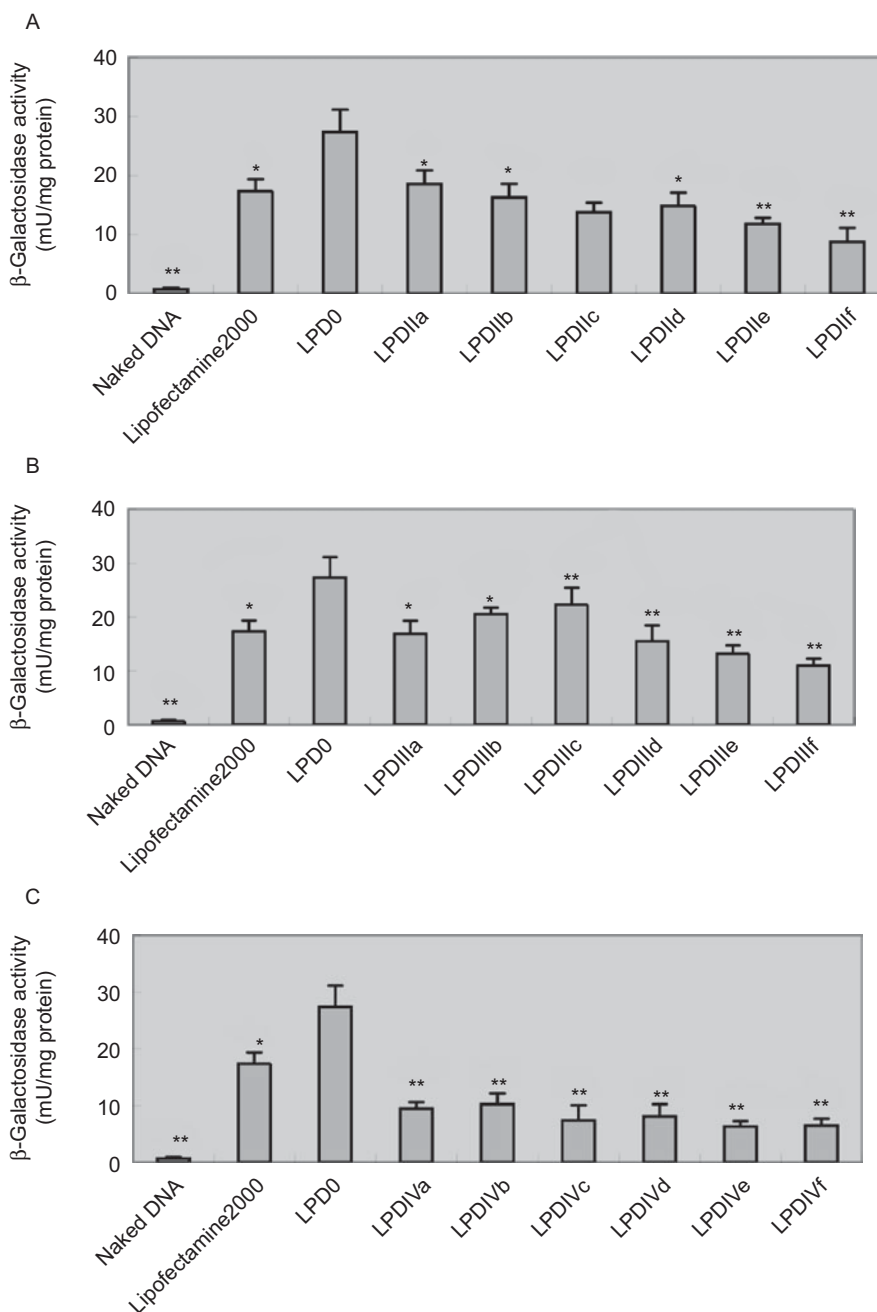


**Figure 6.** Comparison of transfection efficiencies of LPDs and Lipofectamine™ 2000 Transfection Reagent in A549 cells. (A) LPD0, Lipofectamine™ 2000 and LPDIIa-f, (B) LPD0, Lipofectamine™ 2000 and LPDIIIa-f, (C) LPD0, Lipofectamine™ 2000 and LPDIVa-f. Transfect efficiency was compared between LPD with the highest transfect ability (LPD0) and other LPDs as well as Lipofectamine™ 2000 within each group. The data points represent the mean  $\pm$  SD of three experiments ( $P < 0.05^*$ ,  $P < 0.01^{**}$ ). The transfect efficiency in A549 cells did not increase using LPDs bearing galactose residues compared with LPD0.

into HepG2 cells in contrast to the control group LPD0 ( $P > 0.05$ ) (Figure 7).

#### Galactose competitive inhibition assay

To further validate the recognition of galactosidase residues of LPDs by the ASGP-R, galactose competitive inhibition assay was carried out on LPDIIb, LPDIIIc, and

LPDIVE, each of which performed the highest transfect efficiency to HepG2 cells within the same galactose density group. As demonstrated in Figure 8, the transfect activities of LPDIIb, LPDIIIc and LPDIVE can be significantly inhibited at the presence of 80 mmol galactose ( $P < 0.05$ ), while the existence of mannose at the same concentration failed to suppress their gene transfer. In addition, the inhibition effect by galactose was slightly

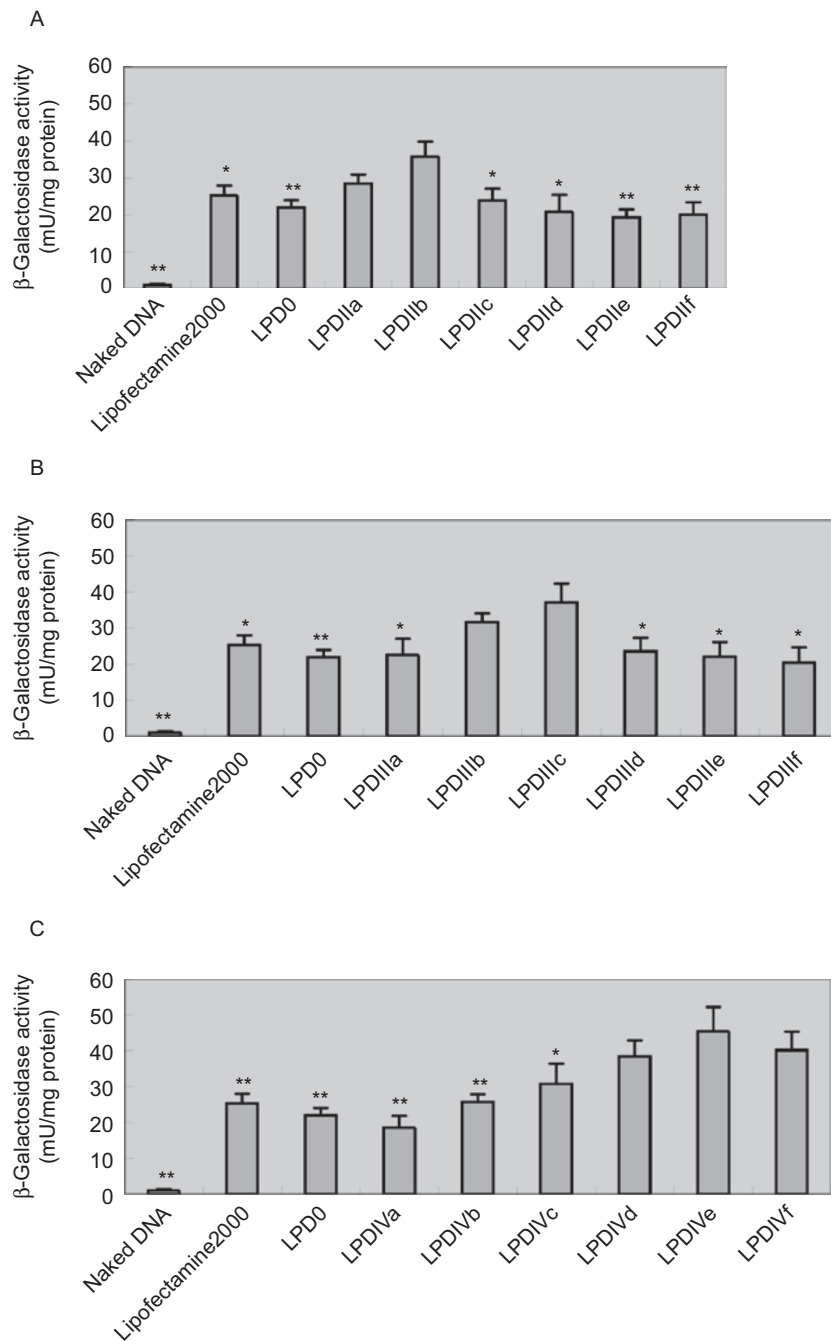


**Figure 7.** Comparison of transfection efficiencies of LPDs and Lipofectamine™ 2000 Transfection Reagent in HepG2 cells. (A) LPD0, Lipofectamine™ 2000 and LPDIIa-f; (B) LPD0, Lipofectamine™ 2000 and LPDIIIa-f; (C) LPD0, Lipofectamine™ 2000 and LPDIVa-f. Transfect efficiency was compared between LPD with the highest transfect ability (A: LPDIIb, B: LPDIIIc, C: LPDIVE) and other LPDs as well as Lipofectamine™ 2000. The data points represent the mean  $\pm$ SD of three experiments ( $P < 0.05^*$ ,  $P < 0.01^{**}$ ). LPDIIa-b, LPDIIIb-c, and LPDIVd-f performed significant higher transfect efficiencies in HepG2 cells.

enhanced in LPDs with more galactose residues, but without significant difference ( $P > 0.05$ ). Taken together, these results were in accordance with *in vitro* gene transfer studies into HepG2 and A549 cells, validating

the specific recognition of galactose residues of LPDs by ASGPR on the surface of HepG2 cells and the strengthened affinity between the ASGPR and the ligand with more galactose residues.

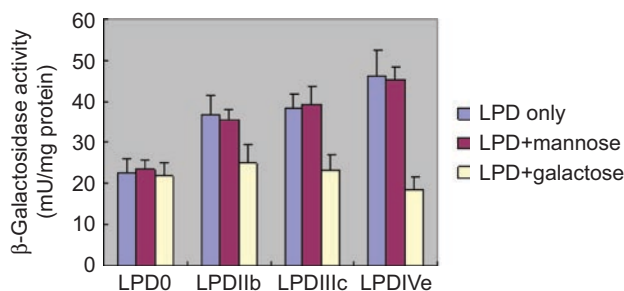


**Figure 8.** Galactose competitive inhibition assay. Effects of mannose or galactose (80 mM) on the transfection activities of LPDIIB, LPDIIIc, and LPDIVE in HepG2 cells. The data points represent the mean  $\pm$ S.D. of three experiments. Cells were seeded at  $2 \times 10^5$  cells/well onto 12-well plates 24 h before transfection. After the cells were washed twice by PBS, 0.5 mL serum and antibiotics-free medium were added into each well. For each well, LPD containing 4  $\mu$ g pORF-1acZ, LPD/80 mM D-galactose or LPD/80 mM D-mannose were diluted to 0.5 mL by the serum-free medium, and then gently overlaid onto the cells. After incubation of 6 h, medium were moved and cells were washed twice with PBS, then the transfection efficiency was measured by  $\beta$ -galactosidase assay.

### Cytotoxicity assay

Since the toxicity of nonviral cationic vectors may interfere with their transfection activities, the relative viabilities of two cell types (HepG2 and L929) after exposure to LPDs with the DNA concentration of 4 mg/mL was measured by MTT method, in contrast to the control group LPD0. Figure 9 shows all the Gal-LPDs presented no obvious toxicities to L929 cell line and HepG2 cell line. Moreover, they did not have significant difference ( $P < 0.05$ ) in toxicity between each other.

### Discussion

Our present study aims to further elucidate how structural differences of the galactose ligands on the gene transfer vector LPD influence the transfect ability by affecting the binding affinity between the ligands and the receptor ASGPR. Previous structure-activity studies of synthetic galactosides and isolated oligoantennary glycopeptides with the asialoglycoprotein receptor have provided some insight into the basic structural requirements for ligand recognition. The nature of the branching pattern of the oligosaccharide component as well as the distance between the galactosyl residues were suggested to be major factors determining the affinity of a ligand (Lee et al., 1983; Baenziger & Maynard, 1980; Kawaguchi et al., 1980; Connolly et al., 1982; Lee, Lin, & Lee, 1984). Therefore, to illuminate the effects of these factors on transfect activity, we synthesized a series of cluster ligands varying in galactose substitution degree and spacer lengths of the cholesterol derivatives by virtue of a flexible chemical strategy which allows for the preparation

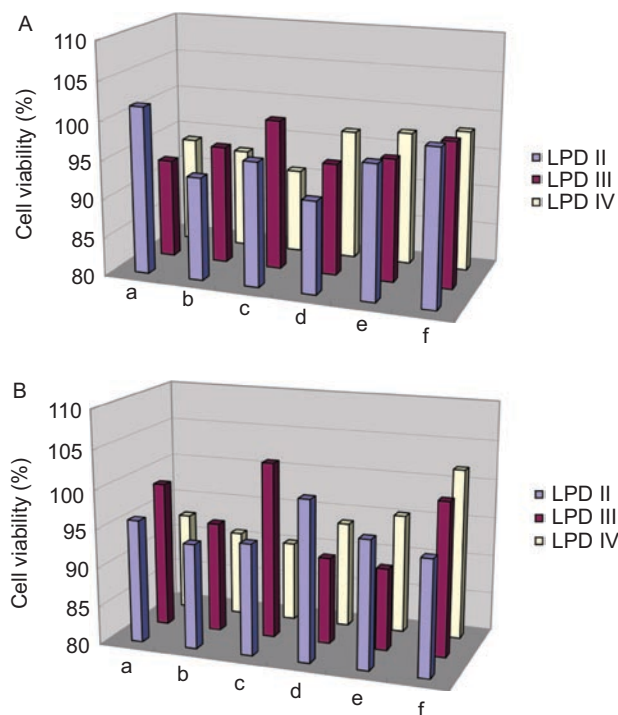


**Figure 9.** Cytotoxicity assay. Cytotoxicity of LPDs in (A) L929, (B) HepG2 cell lines were measured by MTT test. Cells were plated at 15,000 cells/well into 96-well plates one day before transfection. Then cells were transfected using LPDs. After incubation of 45 h, cell viability was measured by MTT test. Data are means of three experiments (SD < 10%).

of multi-antennary galactosyl ligands, differing in their inter-galactose distances.

It is well recognized that the mode of formation of the lipoplexes strongly determines the final physicochemical characteristics of the lipoplexes, including size, charge, density and colloidal stability, which consequently modulates their biological activity both *in vivo* and *in vitro* (Pedroso et al., 2001). Therefore, it is of crucial importance to optimize the formulation of lipid-polycation-DNA complexes as well as characterize these parameters that govern transfection profiles. In the LPD characterization assay, we determined the zeta potential and particle size of LPDs. As shown in Table 1, the particle size of these LPDs briefly increased with more galactose residues (LPDIVE > LPDIIIc > LPDIIB). This might be attributed to a shielding effect on part charges by galactose residues, which leads to the increase of the hydrophilicity of Gal-LPD, resulting in enhanced hydration and thus cause the size to increase.

In cell transfection studies, we measured  $\beta$ -galactosidase activity in both A549 and HepG2 cells. As indicated in Figure 7, LPDIIB, LPDIIIc, and LPDIVE exhibited higher transfect efficiency compared with LPD0 and lipofectamine™ 2000 in HepG2 cells whereas the transfect activity in A549 cells decreased using LPDs containing cholesterylated thiogalactosides, in contrast

to the control group LPD0. This can be rationalized by the receptor mediated internalization. ASGPR, highly expressed on the surface of HepG2 cells, can recognize galactosidase residues of cholesterylated thiogalactosides and therefore facilitate the internalization of LPD into HepG2 cells. However, the human alveolar epithelial cell line A549 cell lacks ASGPR; moreover, the presence of galactose residues may cause an enhanced surface hydrophilicity and facilitate the formation of water shell to the surfaces of galactosylated LPDs, which was hypothesized to hinder the membrane fusion and consequently suppressed the gene expression of galactosylated LPDs in A549 cells. Besides, it is quite obvious that regarding the gene transfer ability, LPDIVE > LPDIIIc > LPDIIb. This is in consistent with previous research by Reiko T. Lee et al., which has established each addition of a galactosyl residue to an existing ligand structure invariably increased the binding affinity of such a ligand (Lee, Lin, & Lee, 1984). And according to Kawasaki et al., multivalent ligands showed a strong "cluster effect," which is defined as affinity enhancement over and beyond what would be expected from the concentration increase of the determinant sugar in a multivalent ligand and geometries (Balaji et al., 1993). Therefore, for those LPDs bearing optimized spatial arrangement and restricted geometry, the increase in galactose densities undoubtedly improved the ligand's binding affinity, leading to enhanced gene delivery into hepatocytes.

Also, it is notable that among those Gal-LPDs, including LPDIIa, LPDIIc-f, LPDIIIa, LPDIIIId-f, LPDIVa-c, though bearing higher galactose densities than LPD0, did not significantly increase the transfect efficiency into HepG2 cells. This can be explained by unoptimized spacer lengths. At a given level of valency, the binding strength of a cluster ligand depended mainly on two factors: (1) the maximum spatial inter-galactose distances and (2) the flexibility of the arm connecting galactosyl residues and the branch points (Lee, Lin, & Lee, 1984). Moreover, optimal interactions with the clustered galactosides ("cluster effect") also require well defined inter-galactose distances (Lee, Lin, & Lee, 1984) and geometries (Ozaki et al., 1995). Furthermore, previous work has established a model in which only glycopeptides bearing terminal Gal or GalNAc residues that fall within a restricted spatial relationship can induce a conformational alteration in the receptor which is required for uptake to occur and the spacing of terminal Gal and GalNAc residues is critical for interaction with the lectin binding site and that this would be reflected in the susceptibility of these glycopeptides to endocytosis (Baenziger & Fiete, 1980). As a consequence, LPDIIa, LPDIIc-f, LPDIIIa, LPDIIIId-f, LPDIVa-c, which lack the proper dimensions for the binding to the receptor, presented relatively weak gene transfer ability. By contrast,

LPDIIb, LPDIIIc, and LPDIVE, which attain appropriate spatial and conformational arrangement for the tight binding to the receptor, exhibited superior gene transfer ability to HepG2 cells.

In conclusion, we have established LPDIVE, LPDIIIc, and LPDIIb, bearing the most appropriate inter-galactose distances were the most sufficient gene transfer vector at each given level of valency, with low toxicity. And regarding the substitution degree of galactose residues, under optimized spatial arrangement, the gene transfer ability was: tetra- > tri- > mono-antennary galactose contained LPDs. Therefore, our work would prove valuable for future research in optimizing the strategy for hepatotrophic gene targeting.

## Declaration of interest

We are thankful for the financial support of the National Natural Science Foundation of China (Grant No: 30600786).

## References

- Baenziger JU, Fiete D. (1980). Galactose and N-acetylgalactosamine-specific endocytosis of glycopeptides by isolated rat hepatocytes. *Cell* 22: 611-620.
- Baenziger JU, Maynard Y. (1980). The asialoglycoprotein receptor. *J Biol Chem* 255: 4607-4613.
- Balaji PV, Qasba PK, Rao VS. (1993). Molecular dynamics simulations of asialoglycoprotein receptor ligands. *Biochemistry* 32:12599-12611.
- Bider MD, Wahlberg JM, Kammerer RA, Spiess M. (1996). The oligomerization domain of the asialoglycoprotein receptor preferentially forms 2:2 heterotetramers *in vitro*. *J Biol Chem* 271: 31996-32001.
- Bock K, Arnarp J, Lönngrén J. (1982). The preferred conformation of oligosaccharides derived from the complex-type carbohydrate portions of glycoproteins. *Eur J Biochem* 129: 171-178.
- Burns CJ, Field LD, Hashimoto K, Petteys BJ, Ridley DD, Samankumara Sandanayake KRA. (1999). A convenient synthetic route to differentially functionalized long chain polyethylene glycols. *Synth Commun* 29: 2337-2347.
- Connolly DT, Townsend RR, Kawaguchi K, Bell WR, Lee YC. (1982). Binding and endocytosis of cluster glycosides by rabbit hepatocytes. Evidence for a short-circuit pathway that does not lead to degradation. *J Biol Chem* 257: 939-945.
- Eggers I, Fenderson B, Toyokuni T, Dean B, Stroud M, Hakomori S. (1989). Specific interaction between Lex and Lex determinants. A possible basis for cell recognition in preimplantation embryos and in embryonal carcinoma cells. *J Biol Chem* 264: 9476-9484.
- Gao X, Huang L. (1996). Potentiation of cationic liposome-mediated gene delivery by polycations. *Biochemistry* 35: 1027-1036.
- Horejsi V, Smolek P, Kocourek J. (1978). Studies on lectins. XXXV. Water-soluble O-glycosyl polyacrylamide derivatives for specific precipitation of lectins. *Biochim Biophys Acta* 538: 293-298.
- Hukkamaki J, Pakkanen TT. (2001). Study on catalytic hydrogenation in synthesis of four-directional amine-terminated dendritic molecules. *Journal of molecular catalysis. A, Chemical*. 174: 205-211.
- Kawaguchi K, Kuhlenschmidt M, Roseman S, Lee YC. (1980). Synthesis of some cluster galactosides and their effect on the hepatic galactose-binding system. *Arch Biochem Biophys* 205: 388-395.

- Khorev O, Stokmaier D, Schwardt O, Cutting B, Ernst B. (2008). Trivalent, Gal/GalNAc-containing ligands designed for the asialoglycoprotein receptor. *Bioorg Med Chem* 16: 5216–5231.
- Lee RT, Lin P, Lee YC. (1984). New synthetic cluster ligands for galactose/N-acetylgalactosamine-specific lectin of mammalian liver. *Biochemistry* 23: 4255–4261.
- Lee YC, Townsend RR, Hardy MR, Lönngren J, Arnarp J, Haraldsson M, Lönn H. (1983). Binding of synthetic oligosaccharides to the hepatic Gal/GalNAc lectin. Dependence on fine structural features. *J Biol Chem* 258: 199–202.
- Li S, Rizzo MA, Bhattacharya S, Huang L. (1998). Characterization of cationic lipid-protamine-DNA (LPD) complexes for intravenous gene delivery. *Gene Ther* 5: 930–937.
- Li S, Huang L. (1997). *In vivo* gene transfer via intravenous administration of cationic lipid-protamine-DNA (LPD) complexes. *Gene Ther* 4: 891–900.
- Loiseau FA, Hii KK, Hill AM. (2004). Multigram synthesis of well-defined extended bifunctional polyethylene glycol (PEG) chains. *J Org Chem* 69: 639–647.
- Masotti A, Mossa G, Cametti C, Ortaggi G, Bianco A, Grosso ND, Malizia D, Esposito C. (2009). Comparison of different commercially available cationic liposome-DNA lipoplexes: Parameters influencing toxicity and transfection efficiency. *Colloids Surf B Biointerfaces* 68: 136–144.
- Meier M, Bider MD, Malashkevich VN, Spiess M, Burkhard P. (2000). Crystal structure of the carbohydrate recognition domain of the H1 subunit of the asialoglycoprotein receptor. *J Mol Biol* 300: 857–865.
- Newkome GR, Mishra A, Moorefield CN. (2002). Improved synthesis of an ethereal tetraamine core for dendrimer construction. *J Org Chem* 67: 3957–3960.
- Nikken W, Yen WT, Yi YY. (2009). Targeted co-delivery of drug and gene with self-assembled galactosylated amphiphilic oligopeptide nanostructures for cancer treatment.
- Ozaki K, Lee RT, Lee YC, Kawasaki T. (1995). The differences in structural specificity for recognition and binding between asialoglycoprotein receptors of liver and macrophages. *Glycoconj J* 12: 268–274.
- Pazur JH. (1981). Affinity chromatography of macromolecular substances on adsorbents bearing carbohydrate ligands. *Adv Carbohydr Chem Biochem* 39: 405–447.
- Pedroso de Lima MC, Simões S, Pires P, Faneca H, Dúzquines N. (2001). Cationic lipid-DNA complexes in gene delivery: from biophysics to biological applications. *Adv Drug Deliv Rev* 47: 277–294.
- Roy R, Tropper FD, Romanowska A. (1992). New strategy in glycopolymer syntheses. Preparation of antigenic water-soluble poly(acrylamide-co-p-acrylamido-Phenyl.beta.-lactoside). *Bioconjugate Chem* 3: 256–261.
- Schwartz AL, Fridovich SE, Knowles BB, Lodish HF. (1981). Characterization of the asialoglycoprotein receptor in a continuous hepatoma line. *J Biol Chem* 256: 8878–8881.
- Sorgi FL, Bhattacharya S, Huang L. (1997). Protamine sulfate enhances lipid-mediated gene transfer. *Gene Ther* 4: 961–968.
- Stowell CP, Lee VC. (1980). Neoglycoproteins: the preparation and application of synthetic glycoproteins. *Adv Carbohydr Chem Biochem* 37: 225–281.
- Stoll MS, Mizuochi T, Childs RA, Feizi T. (1988). Improved procedure for the construction of neoglycolipids having antigenic and lectin-binding activities, from reducing oligosaccharides. *Biochem J* 256: 661–664.
- Sun X, Hai L, Wu Y, Hu HY, Zhang ZR. (2005). Targeted gene delivery to hepatoma cells using galactosylated liposome-polycation-DNA complexes (LPD). *J Drug Target* 13: 121–128.